

When higher carrying capacities lead to faster propagation:

Supplementary Information

1 S1: Growth functions for strong Allee effects

Here we depict the growth functions f with different values of K . Fig. 1 depicts the standard one in (1):

$$f(u) = r u (1 - u/K) (u - \rho), \quad (1)$$

with the maximal per capita growth rate increasing with the increase of K . Fig. 2 depicts the new function defined by (2), with the maximal per capita growth rate independent of K :

$$f(u) = 4r \frac{K}{(K - \rho)^2} u (1 - u/K) (u - \rho). \quad (2)$$

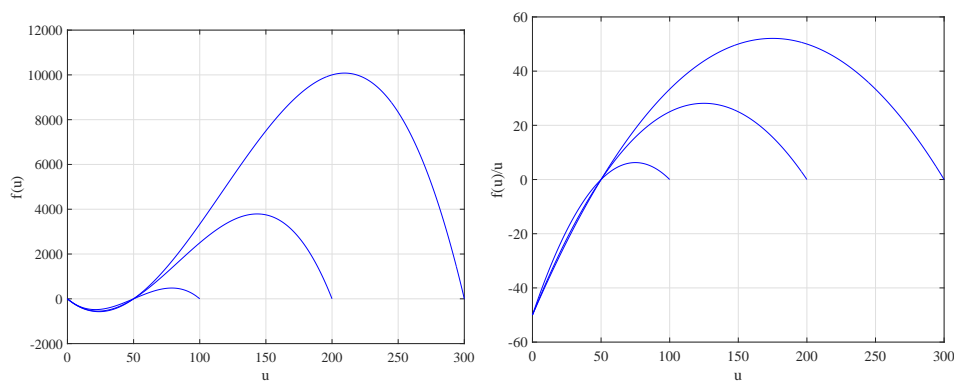


Figure 1: Left: the growth function f given by the classical formula (1), for $K = 100, 200, 300$ and $r = 1, \rho = 50$. Right: the corresponding per capita growth rate $f(u)/u$

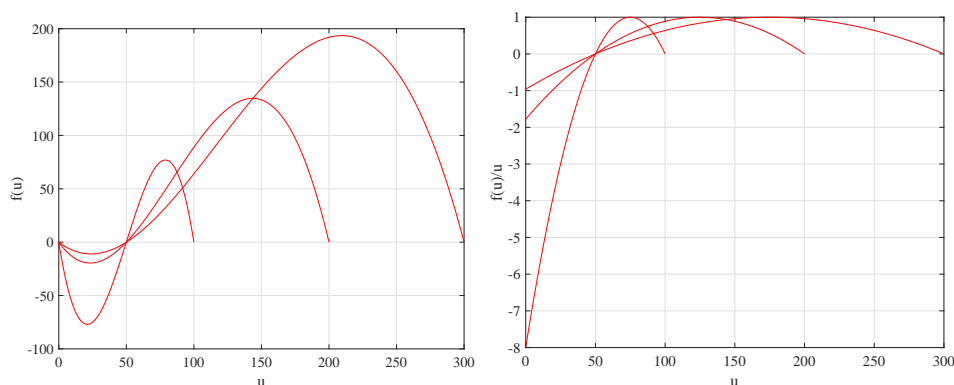


Figure 2: Left: the growth function f given by the new formula (2), for $K = 100, 200, 300$ and $r = 1, \rho = 50$. Right: the corresponding per capita growth rate $f(u)/u$

2 S2: Presence of density-dependent dispersal

In order to investigate the presence of density-dependent dispersal in our dataset, we performed an Approximate Bayesian Computation (ABC) with the software R. Since we know that there is no Allee effect in *T. chilonis* populations under these experimental conditions (Morel-Journel et al., 2016), we focused on fixed dispersal and positive density-dependent dispersal scenarios. For this analysis, our dataset was summarized by 576 pairs of patches from the front $(N_i(t), N_{i+1}(t+1))$, where $N_i(t)$ is the number of individuals in the patch i at generation t and $N_{i+1}(t+1)$ is the population size in the next patch at time $t+1$. Those data come from our main experiment previously described in the article. We compared two scenarios, each one corresponding to a different dispersal type. Each scenario was run 500000 times. We chose as summary statistics the maximal number of parasitized eggs on the edge patch on the 576 couples, the total number of parasitized eggs on the 576 edge patches, the number of empty edge patches, and the number of edge patches with [1:50] parasitized eggs.

For the first scenario (fixed dispersal), we began by drawing the probability of dispersal in the next patch p and the mean number of offspring per female R in uniform distributions: $p \sim \mathcal{U}(0, 1)$ and $R \sim \mathcal{U}(0, 30)$. Then,

$$N_{i+1}(t+1) = \sum_{j=1}^{N_i(t)} p_j r_j,$$

where $p_j \in \{0, 1\}$ follows a Bernoulli distribution with probability $p/2$, namely the probability of being a female ($1/2$) and to disperse in the next patch (p). The number of offsprings r_j follows a Poisson distribution with parameter R : $r_j \sim \text{Poisson}(R)$.

For the second scenario (positive density-dependent dispersal), only the dispersal part was changed and was based on a sigmoid-like dependence via a Hill function:

$$p_j = \frac{N_i(t)}{\tau + N_i(t)},$$

where τ follows a uniform distribution over an interval such that the minimal probability of dispersal is equal to 0.01 and the maximal probability of dispersal is equal to 0.2 for a population of 500 individuals.

To select the best model, we used the R package *abc* (Csilléry et al., 2012). First we ensured, with a cross validation, that our models were sufficiently different for the analysis to discriminate between them.

The ABC analysis showed a clear positive result for the positive density-dependent migration model,

chosen at 100% against the density-independent migration model.

3 S3: Experimental vs simulation results

Using the IBM with positive density-dependent dispersal, we adjusted the parameter value R so that the mean number of colonized patches after 10 generations was consistent with the experimental results of Section "Experimental study: propagation of a parasitoid wasp in a microcosm" for large K (modality L in the experimental study and $K = 400$ in the simulation model). The value of the parameter p_1 was sampled from a uniform distribution in $(0, 0.04)$, consistently with the posterior mode found with the ABC approach (0.02, see Supplementary Information S2 for more details regarding the ABC approach). Then, using the same parameter values, we computed the mean number of colonized patches over 10 generations for "very small" ($K = 70$) and "small" ($K = 200$) carrying capacities. The results are presented in Fig. 3a. Consistently with our experimental results, the differences between the small and large modalities are minor during the the first 10 generations. The effect of K is more visible over the first 10 generations if we compare the large and very small modalities.

If we focus on the dynamics with small and large K modalities during the first 10 generations, we observe 3 different stages: during the first generations, the two modalities lead to the same dynamics; then during a second stage the largest modality leads to a slightly faster colonization; during the last stage, the two modalities lead to comparable speeds. The existence of these 3 stages is consistent with the experimental results (Fig. 3a).

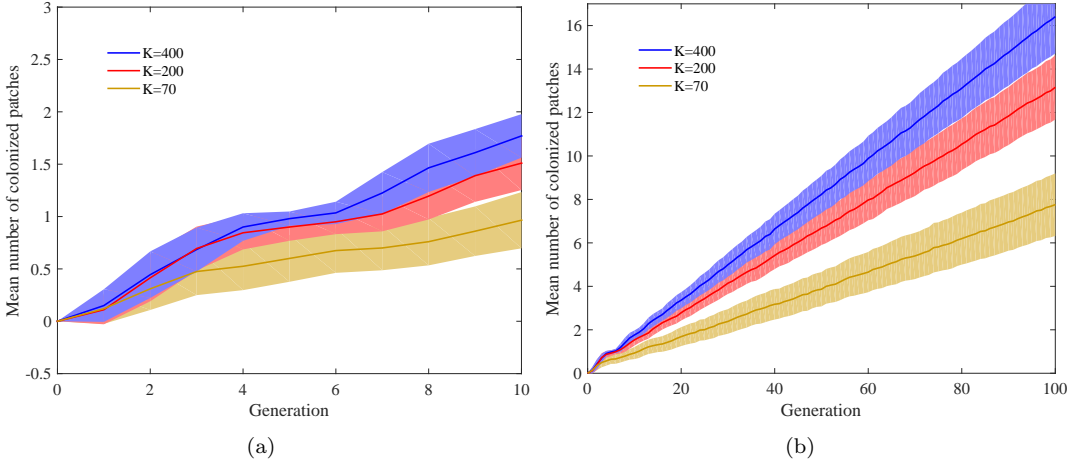


Figure 3: Simulation results: effect of K on the mean number of colonized patches during the first 10 generations (a) and 100 generations (b). We used the IBM with positive density-dependent dispersal. The probability of migration p_1 was sampled from a uniform distribution in $(0, 0.04)$ and $R = 1.7$. The number of individuals inoculated in the first patch was always equal to 50. The mean values are computed over 200 replicates. The shaded regions correspond to mean 95% confidence intervals obtained over 10 replicates of 20 simulations.

With the parameter values used here (see the legend of Fig. 3), the asymptotic speeds after large time are 0.09 ($K = 70$), 0.14 ($K = 200$) and 0.17 ($K = 400$) patch per generation. Thus, if the experimental results remain consistent with the simulation model, we expect increasing differences between the different modalities at large times (Fig. 3b).

4 S4: Very small carrying capacity

Another experiment with a very small K with 70-90 host eggs (Modality VS), which we conducted for another purpose, led to new results that strongly support our conclusions. In spite of a slightly different experimental protocol, we believe that these results can be compared to those in the main text, see Fig 4. The main differences in the experimental protocol are presented in the Table 1. In order to compare the three modalities, we plotted the very small modality from the third generation to account for the time to reach carrying capacity in the other modalities.

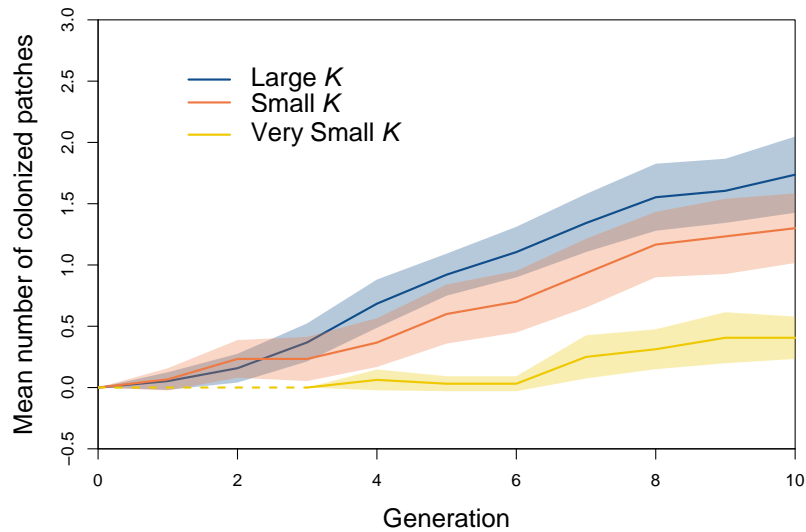


Figure 4: Mean number of colonized patches over the 38 replicated populations for modality L, 30 for the modality S, and 32 for the modality VS. The yellow line corresponds to the very small carrying capacity 70-90 host eggs, red line corresponds to the small carrying capacity 150-200 host eggs, and the blue line corresponds to the large carrying capacity 400-450 host eggs. Envelopes around the lines represent the 95% confident interval.

	Experiment 1	Experiment 2
Maintenance conditions and life cycle		
Night and day time	16h day/8h night	
Humidity	around 70%	
Life cycle	last 9 days	last 15 days
Temperature	25°C	20°C
Host eggs	<i>Ephestia kuehniella</i>	
Experimental system		
Landscape Size	11 patches	7 patches
Initial colonized patches	1	4
Location of initial colonized patches	middle	both edges
Number of individuals inoculated	50	K (70-90)
Spatial dynamics	spread on both sides from the middle patch	spread from the edges, filling the middle gap
Time for dispersal/reproduction	2 days	

Table 1: Table of similarities and differences between the main experiment presented in this paper (Experiment 1) and the posterior experiment with a very small carrying capacity modality (Experience 2).

References

- Csilléry, K., O. François, and M. G. Blum (2012). abc: an r package for approximate bayesian computation (abc). *Methods in ecology and evolution* 3(3), 475–479.
- Morel-Journel, T., P. Girod, L. Mailleret, A. Auguste, A. Blin, and E. Vercken (2016). The highs and lows of dispersal: how connectivity and initial population size jointly shape establishment dynamics in discrete landscapes. *Oikos* 125(6), 769–777.